Analytical Approach to Base Station Sleep Mode Power Consumption and Sleep Depth

Oluwakayode Onireti*, Abdelrahim Mohamed†, Haris Pervaiz† and Muhammad Imran*
*School of Engineering, University of Glasgow, Glasgow, UK
†Institute for Communication Systems ICS, University of Surrey, Guildford, UK
Email: oluwakayode.onireti@glasgow.ac.uk

***Abstract*—In this paper, we present an analytical framework to model the sleep mode power consumption of a base station (BS) as a function of its sleep depth. The sleep depth is made up of the BS deactivation latency, actual sleep period and activation latency. Numerical results demonstrate a close match between our proposed approach and the actual sleep mode power consumption for selected BS types. As an application of our proposed approach, we analyze the optimal sleep depth of a BS, taking into consideration the increased power consumption during BS activation, which exceeds its no-load power consumption. We also consider the power consumed during BS deactivation, which also exceeds the power consumed when the actual sleep level is attained. From the results, we can observe that the average total power consumption of a BS monotonically decreases with the sleep depth as long as the ratio between the actual sleep period and the transition latency (deactivation plus reactivation latency) exceeds a certain threshold.**

***Index Terms*—Average power consumption; base station; power consumption model; sleep depth; transition latency.**

I. Introduction

The fifth generation (5G) of cellular networks will be characterized by tremendous growth and dynamism in user access technique and data traffic [1], [2]. In order to support the expected 5G evolution in an economic and ecological viable manner, the power consumption in mobile cellular networks should be minimized. A breakdown of the power consumption of the mobile cellular network reflects that about 80% of the total power is consumed by the base stations (BSs) [3]. Hence, most optimization effort towards maintaining power consumption evolution in 5G cellular networks has been on the BS. An accurate power consumption model is a prerequisite for such optimization.

In [4], the authors presented a linear power consumption model for the BS, which takes into account the signal processing power, amplifier inefficiency, and power losses. The power consumption of extra BS components such as the alternating current (AC)- direct current (DC) converters and DC-DC converters, cooling and power supply losses have been considered in [5], [6]. The latter work shows that the relationship between the transmit power and the BS power consumption is nearly linear. A more advanced flexible power consumption model, which is based on a combination of the BS's components and subcomponents as well as power scaling rules as functions of system parameters such as bandwidth, spectral efficiency, number of antennas, system load, number of spatial streams and quantization, has been recently proposed in [7]–[9]. The relaxed constraints for BS on/off operation in the control and data separation architecture [10], which is a candidate architecture for 5G networks, mean that accurate modeling of the sleep mode power consumption is also very essential for evaluating the energy saving gain of this architecture.

The BS still consumes a significant amount of power when in the idle mode, i.e., not transmitting data, since all of its components are still active. Energy proportionality with traffic, which is an essential target for 5G cellular networks, implies that a BS with no-load should have zero or very low power consumption. With the partial deactivation of the BS's components/subcomponents, a BS can enter into a lower power consumption mode. However, BSs usually need a longer activation time when operating in the low power consumption mode, which could have a significant impact on the quality of service (QoS). Short activation time can only be guaranteed if a number of components of the BS hardware, which take a non-negligible time to be switched on, stay on even when the BS is in sleep mode. Hence, the current state of the art BSs have to utilize higher power consumption in sleep mode in order to guarantee the QoS [6], [11], resulting into an energy/delay tradeoff. Nevertheless, deeper sleep levels can be achieved in BSs by exploiting the flexibility of the network in addition to the hardware capability. Traffic can be offloaded to neighboring BS(s) in the case of homogeneous deployment and overlapping cells in heterogeneous deployment. In [9], the authors identified four different sleep depth with different transition times and power savings based on the hardware capability and network flexibility. By using queuing theory, the authors of [12], [13] presented the average power consumption of a BS in sleeping mode. However, fixed sleep power savings was considered during the BS sleeping and set-up phases. In this paper, we present an analytical framework that models the sleep mode power consumption of the BS

TABLE I
BASE STATION POWER CONSUMPTION [W] IN 2020 TECHNOLOGY AND SLEEP DEPTH τ [9], [14]

BS power Consumption	Load		Sleep Mode			
	Full	None	1	2	3	4
			71.4 μs	1 ms	10 ms	1 s
4×4 macro	742.2	139	86.3	12.3	7.23	6.16
2×2 macro	702.6	115	76.5	8.56	6.02	5.27
pico	6.9	2.16	1.51	0.368	0.301	0.238
femto	2.2	0.966	0.641	0.221	0.187	0.125

as a function of its sleep depth. The latter is made up of the BS's subcomponent/component deactivation and activation latencies, and the actual sleep period. This proposed model allows for flexibility in the sleep level as against the four discrete sleep levels in [9], [14]. Using the proposed analytical model, we derive the average power consumption and analyze the optimal sleep depth of the BS, taking into consideration the activation and deactivation cost. This paper is organized as follows. In section II, we introduce the BS sleep modes. In section III, we describe our system model. In section IV, we model the power consumption at the various phases. We also present the optimization of the sleep duration. In section V, we present some numerical results. Finally, section VI concludes the paper.

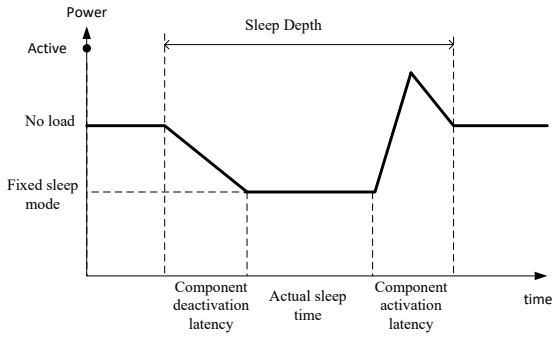

Fig. 1. Base station transition latency showing component deactivation latency, actual sleep period and activation latency.

II. BASE STATION SLEEP MODES

Power consumption models such as the EARTH and GreenTouch models [6], [9] have shown that significant amount of power is consumed when the BS is not loaded with data, i.e., idle. In the idle mode, power consumption reduction is minimal since the BS hardware component remains completely active. In order to achieve lower power consumption, partial deactivation of the BS's components has been proposed. However, with the partial deactivation of the BS's components, information on hardware (BS component) capability such as power savings and transition latencies, and the flexibility of the network are required. Furthermore, different sleep levels corresponding to different sleep depth has been identified in [9]. The sleeping modes correspond to sleep depth of 71 μs (LTE OFDM symbol), 1 ms (LTE subframe), 10 ms (LTE radio frame) and 1 s (long term sleep). Table I shows the power consumed at different sleep depth based on hardware characteristics and for various BS types.

In a sleep mode, all components with transition latency (deactivation plus reactivation latency) shorter than the sleep depth will be considered sleeping, while components with longer transition latency will be considered active. Hence, as shown in Fig. 1, the sleep depth entails the component deactivation latency, actual sleep time and component activation latency. Therefore, the actual time interval at which the BS operate at the sleep level is less than the sleep depth. Note that the power consumed during the activation and deactivation times are much higher than the power consumed during the actual sleep level [15], [16]. For the sleep mode 1, with a sleep depth of 71 μs the small signal blocks considered for deactivation have to show a deactivation latency shorter than the 17 μs limit defined in [17] for the transmitter transient period [18]. This applies to the activation latency as well. Hence, in a realistic scenario, the sum of the activation and deactivation latencies must be less than the actual sleep period.

III. SYSTEM MODEL

In this paper, we focus our analysis on the average power consumption of a typical BS which can be considered as a single server. This represents a higher level abstraction of the network such that the flow-level sessions like web page downloads from the BS are the tasks. The task (traffic) arrival process is assumed to be a Poisson process with arrival rate λ, with each task requiring an independently and identically distributed (i.i.d) service time B, which follows a general distribution. We assume that the on-demand activation of the BS is in accordance with the traffic arrival and that the active time distribution is also in accordance with the service time distribution. We consider the service discipline of the server to be a first-come-first-serve (FCFS) discipline. When the queue becomes empty, i.e., the BS has finished serving its users, it waits for a hysteresis time D, which follows a general distribution. If a new task arrive during the hysteresis time, the server/BS[1] will immediately start its service,

[1]Note that we use the terms server and BS interchangeably.

otherwise, it will enter the sleep mode.

For the BS in the sleep mode, we consider the multiple sleep (MS) wake up scheme, where a network controller can detect the network status for each BS after a specific period of time, and wakes the BS up only when there are tasks waiting in the system. Hence, the BS takes a vacation length V if the queue remains empty [12]. The set-up time S, which accounts for the overhead cost, is the sum of the BS's component activation and deactivation latencies. Furthermore, the sleep depth τ is the sum of the set-up time/transition latency[2] S and the vacation time (actual sleep time) V. Note that the activation latency can also denote the warm-up time required before the sleeping BS can provide services. To ensure tractability in our analysis, we have focused on only the BS's active time, vacation time and the set-up time. In the following, we present the power consumption expression at the various phases.

IV. Power Consumption at Different Phases

A. Power Consumed in Active Phase

For active BS, we adopt the flexible power consumption model in [9], which can be expressed as

$$P_A = \sum_{i \in I} P_{i,\text{ref}} \prod_{x \in X} \left(\frac{x_{\text{act}}}{x_{\text{ref}}} \right)^{s_{i,x}} + \kappa P_t \qquad (1)$$

where I denote the set of subcomponents i, X the set of input parameters x each having a reference value x_{ref} and an actual value x_{act}, $s_{i,x}$ is the scaling exponent for subcomponent i with respect to parameter x, $P_{i,\text{ref}}$ is the reference power of subcomponent i, κ quantifies the power amplifier (PA) efficiency and P_t is the output power. The reference scenario assumes 20 MHz single antenna operation, spectral efficiency 6 bps/Hz, full load and 24−bit quantization. Tables I-IV in [9] gives the scaling exponent and reference power consumption of the subcomponents. Typical values of the no-load power consumption, P_{ID}, given for the 2020 technology in [9] are used in our evaluation.

B. Power Consumption at the Sleep Mode

Considering an intelligent self-organised cellular network where the sleeping profile of each BS is known in advance, the power consumption in the sleep mode can be modeled as a function of the sleep depth τ (i.e., deactivation latency plus actual sleep period plus activation latency). The sleep level power consumption for discrete sleep depth of $\tau = 71$ μs (OFDM symbol), 1 ms (sub-frame), 10 ms (frame) and 1 s (long term sleep), has been presented in [9], which is shown previously in Table I. However, this model has some restrictions in the sleeping levels since it only supports four states. In the following, we present an accurate approximation of the sleep mode power consumption, which is also flexible in terms of the sleeping level.

[2]The term set-up time also refers to the transition latency and we use both terms interchangeably.

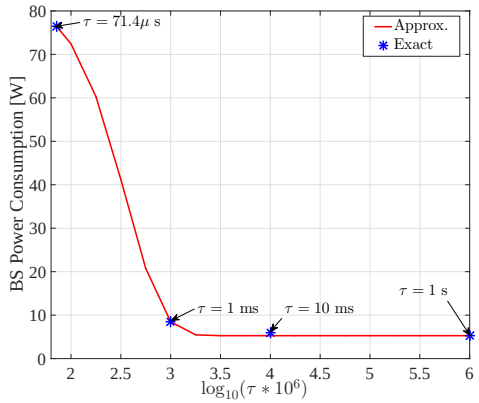

(a) 2×2 macro BS

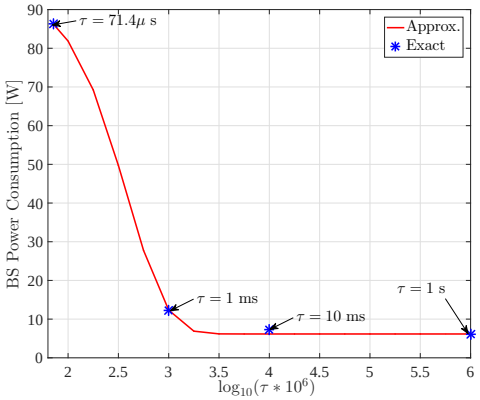

(b) 4×4 macro BS

Fig. 2. Sleep level power consumption approximation as a function of the BS sleep depth τ.

Approximation of the Sleep Mode Power Consumption: In the heuristic curve fitting method proposed in [19], a parametric function is designed in terms of elementary functions and three independent functions for solving a curve fitting problem. In this paper, we utilize this curve fitting method to design the parametric function $\widetilde{P}^i_{SL}(\tau)$ that tightly fits the sleep mode power consumption $P^i_{SL}(\tau)$ for 4×4 macro, 2×2 macro, pico and femto, and for the sleep depth 71 μs $\leq \tau \leq$ 1 s. We use the superscript i to denote the BS type. We first plot sleep power $P^i_{SL}(\tau)$ for $\tau = 71$ μs, 1 ms, 10 ms and 1 s. It can be noticed that $P^i_{SL}(\tau)$ presents a feature of an exponentially decaying function. Note that here we have considered that the sleep mode power consumption $P^i_{SL}(\tau)$ converges to P^i_0, which is the power consumed at the fourth sleep level, for $\tau > 1$ s. In the effort of obtaining the function that best fits the curves in Fig. 2, the curve fitting method leads to the parametric function

$$\widetilde{P}^i_{SL}(\tau) = P^i_m \exp\left(\left(-\omega_1 \log_{10}\left(\tau \times 10^6 \right) \right)^{\frac{1}{\omega_2}} \right) + P^i_0, \qquad (2)$$

TABLE II
PARAMETERS ω_1 AND ω_2 VALUES FOR VARIOUS BS TYPES

	4×4 macro	2×2 macro	pico	femto
ω_1	0.3800	0.3860	0.3920	0.3770
ω_2	0.1350	0.1270	0.1810	0.2110

which provides a satisfying approximation as can be seen in Fig. 2 for 4×4 and 2×2 macro, $\omega_1 = 0.3800, 0.3860$ and $\omega_2 = 0.1350, 0.1270$, respectively. P_m^i is the power consumed by the i^{th} BS type at the fourth sleep level.

C. Power Consumed in the Transition Phase

The transition/set-up phase is made up of the component deactivation and activation phases. We denote the component deactivation and activation latencies by S_D and S_A, respectively. Based on the available measurement in literature, for a given BS component/subcomponent, $S_A > S_D$ [18]. Furthermore, the power consumed at both phases differs. The power consumed during component activation is much greater than the no-load power consumption [15], [16]. Hence, following a similar assumption in [12], we model the power consumed during component activation phase as

$$P_{SA}(\tau) = \beta_1 \left(2P_{ID} - \widetilde{P}_{SL}(\tau)\right) \tag{3}$$

where $\beta_1 \geq 1$ is a system defined parameter and P_{ID} is the no-load power consumption[3]. P_{SA} is a function of the sleep depth and it increases with τ, since higher τ implies that more component/subcomponents will be deactivated and hence a higher activation power consumption. For the deactivation power consumption P_{SD}, we consider it to be a function of the average power consumed over the period of changing from no-load till when the actual sleep level is attained. Hence, we model P_{SD} as

$$P_{SD}(\tau) = \frac{\beta_2}{2}\left(P_{ID} + \widetilde{P}_{SL}(\tau)\right), \tag{4}$$

while assuming a linear decrease in power consumption over this period, where β_2 is a system defined parameter.

D. Average Power Consumption

Assuming deterministic hysteresis time $D = 0$, the average power consumption of the BS while taking into consideration that the system forms a regenerative process [20] satisfies

$$\mathbb{E}[P] = \big(\mathbb{E}[L_A]P_A + \mathbb{E}[L_{SL}][P_{SL}] + \mathbb{E}[L_{SA}]P_{SA} + \mathbb{E}[L_{SD}]P_{SD}\big) / \big(\mathbb{E}[L_A] + \mathbb{E}[L_{SL}] + \mathbb{E}[L_{SA}] + \mathbb{E}[L_{SD}]\big), \tag{5}$$

where L_A, L_{SL}, L_{SA} and L_{SD} denote the length of busy, actual sleep, activation, and deactivation phases, respectively.

The length of time that the regeneration cycle is occupied by the busy phase L_A in the long term average is equivalent to the traffic intensity $\rho = \lambda h_B$, where h_B is the expectation of the service time. The length of the actual sleep, activation and deactivation phases can be obtained as $(1-\rho)h_V$, $(1-\rho)h_{SA}$ and $(1-\rho)h_{SD}$, respectively, where h_V, h_{SA} and h_{SD} are the expectation of V, S_A and S_D, respectively. Consequently, the average power consumption can be simplified as

$$\mathbb{E}[P] = \rho(P_A) + \frac{(1-\rho)(h_V\widetilde{P}_{SL} + h_{SA}P_{SA} + h_{SD}P_{SD})}{h_V + h_{SA} + h_{SD}}. \tag{6}$$

Note that we have considered that the squared coefficient of variation of V to be equal to zero.

E. Optimal Sleep Duration

We consider that the traffic profile is known in advance such that the BS sleep level can be perfectly matched to each vacation period. As a result, short vacation time implies a light BS sleep state while a long vacation time implies a deep BS sleep state. Moreover, we also assume that subcomponents deactivation are done such that subcomponents with short deactivation times[4] are the first to be deactivated. Increasing the BS sleep level implies deactivating more subcomponents, and hence, increasing the deactivation time. This remains the case until when further subcomponent deactivation does not result in change in the sleep depth's power consumption. Hence, in the following sections, we analyze the optimal vacation time for the case where 1) the transition latency/set-up time is proportional to the vacation time and 2) the transition latency is fixed.

1) Transition latency proportional to vacation time: We consider that the transition latency is proportional to the vacation (actual sleep) duration such that

$$\theta = \frac{h_V}{h_{SA} + h_{SD}}. \tag{7}$$

Furthermore, we consider that the activation latency h_{SA} at a particular sleep level is related to the deactivation latency at that sleep level such that

$$\eta = \frac{h_{SA}}{h_{SD}}, \tag{8}$$

where $h_{SA} > h_{SD}$. Consequently, by substituting P_{SA} and P_{SD} in (3) and (4) into (6), the average power consumption can be expressed as a function of the sleep duration such that

$$\mathbb{E}[P] = \rho(P_A) + \frac{(1-\rho)}{(1+1/\theta)}\Big(\widetilde{P}_{SL}(1+Q_1-Q_2) + P_{ID}(Q_1+2Q_2)\Big) \tag{9}$$

where $Q_1 = \frac{\beta_2}{2\theta(\eta+1)}$ and $Q_2 = \frac{\eta\beta_1}{\theta(\eta+1)}$. It can be observed that the average power consumption $\mathbb{E}[P]$ is

[3]We have dropped the superscript i for convenience.

[4]Note that each subcomponent deactivation time is matched to a corresponding activation time

differentiable over its domain such that $\frac{\partial \mathbb{E}[P](h_V)}{\partial h_V}$ can be expressed after simplification as

$$\frac{\partial \mathbb{E}[P](h_V)}{\partial h_V} = \frac{(1-\rho)}{(1+1/\theta)}(1+Q_1-Q2)\frac{\partial \widetilde{P}_{SL}(h_V)}{\partial \tau}\frac{\partial \tau}{\partial h_V} \tag{10}$$

where

$$\frac{\partial \widetilde{P}_{SL}(h_V)}{\partial \tau} = \left[-\frac{\omega_2 P_m e^{-\frac{\left(\omega_1 \ln(\tau \times 10^6)\right)^{\omega_2}}{\ln^{\omega_2}(10)}} \left(\omega_1 \ln(10^6 \times \tau)\right)^{\omega_2}}{\ln^{\omega_2}(10)\tau \ln(10^6 \times \tau)}\right],$$

$\frac{\partial \tau}{\partial h_V} = \frac{\theta+1}{\theta}$ since $\tau = \frac{(\theta+1)h_V}{\theta}$. Note that $\frac{\partial \widetilde{P}_{SL}(h_V)}{\partial h_V}$ is negative over $h_V \in [0, +\infty]$ since ω_1, ω_2 and P_m all take positive real values. Hence, $\frac{\partial \mathbb{E}[P](h_V)}{\partial h_V}$ is strictly decreasing if $(1+Q_1-Q_2) > 0$ and strictly increasing if $(1+Q_1-Q_2) < 0$.

In a realistic scenario, $\theta \geq 1$ and $\eta \geq 1$, hence Q_1 and Q_2 are both less than 1 when the system defined parameters $\beta_1 = \beta_2 = 1$, and thus the differential in (10) will be strictly decreasing. This is desired since increasing the sleep duration leads to a reduction in the overall average power consumption.

Transition latency for constant average power: The average power consumption is a constant function of h_V when $\frac{\partial \mathbb{E}[P](h_V)}{\partial h_V} = 0$ for all h_V in $[0, +\infty]$. The relationship between the transition latency and actual sleep time that achieves such can be obtained by equating $(1+Q_1-Q_2)$ to zero and solving the resulting expression. This latter leads to

$$\theta^\star = \frac{2\eta\beta_1 - \beta_2}{2(\eta+1)}, \tag{11}$$

which is less than 1 when $\beta_1 = \beta_2 = 1$ and $\eta \geq 1$. This implies a transition latency that exceeds the actual sleep duration and is therefore undesirable.

2) Fixed BS transition latency: For the case where the BS transition latency is fixed, the average power consumption expression in (6) can be further expressed as

$$\mathbb{E}[P] = \rho(P_A) + \frac{(1-\rho)\left(\widetilde{P}_{SL}(h_V+Q_3)+Q_4\right)}{h_V+A_0} \tag{12}$$

after substituting P_{SA} and P_{SD} given earlier in (3) and (4), respectively, and the relation $h_{SA} = \frac{\eta A_0}{(1+\eta)}$ and $h_{SD} = \frac{A_0}{(1+\eta)}$, where $A_0 = h_{SA} + h_{SD}$, $Q_3 = \frac{A_0(0.5\beta_2 - \eta\beta_1)}{1+\eta}$ and $Q_4 = \left(\frac{A_0(2\eta\beta_1 + 0.5\beta_2)}{1+\eta}\right) P_{ID}$.

Clearly, $\mathbb{E}[P]$ as defined in (12) is differentiable over its domain, i.e. for $h_V \in [0, +\infty]$, such that $\frac{\partial \mathbb{E}[P](h_V)}{\partial h_V}$ can be expressed after simplification as

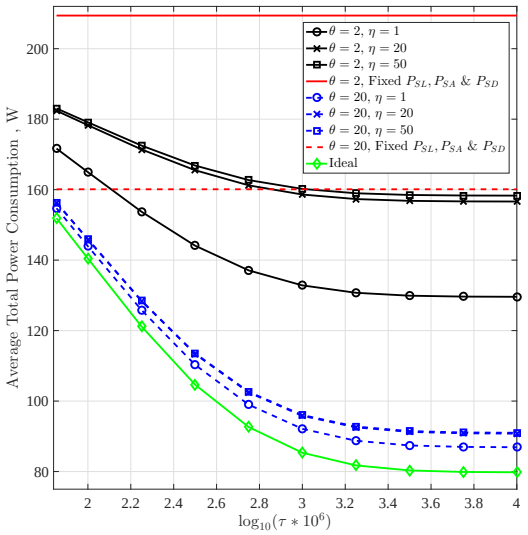

Fig. 3. Effect of the activation and deactivation latencies on the average total power consumption.

$$\frac{\partial \mathbb{E}[P](h_V)}{\partial h_V} = G(h_V) \times \left[\widetilde{P}_{SL}(h_V)(A_0 - Q3) + (h_V + A_0)(h_V + Q3)\frac{\partial \widetilde{P}_{SL}(h_V)}{\partial \tau}\frac{\partial \tau}{\partial h_V} - Q4\right] \tag{13}$$

where $G(h_V) = \frac{1-\rho}{(h_V+A_0)^2} > 0, \tau = h_V + A_0$, $\frac{\partial \tau}{\partial h_V} = 1$. Let $h_V^\star$ be the solution of the equation relating to $\frac{\partial \mathbb{E}[P](h_V)}{\partial h_V} = 0$. Then $\frac{\partial \mathbb{E}[P](h_V)}{\partial h_V} \geq 0$ and $\frac{\partial \mathbb{E}[P](h_V)}{\partial h_V} \leq 0$ for any $h_V \in [0, h_V^\star]$ and $[h_V^\star, +\infty]$, respectively, which in turn means that $\mathbb{E}[P]$ increases over $h_V \in [0, h_V^\star]$ and it decreases over $h_V \in [h_V^\star, +\infty]$. Consequently for fixed transition latency, $\mathbb{E}[P]$ has a unique maximum, which occurs at $h_V = h_V^\star$. Setting $\frac{\partial \mathbb{E}[P](h_V = h_V^\star)}{\partial h_V} = 0$ in (13), we obtain that

$$g(h_V^\star) = P_{SL}(h_V)(A_0 - Q3) + (h_V + A_0)(h_V + Q3)\frac{\partial P_{SL}(h_V)}{\partial \tau} = Q_4, \tag{14}$$

which unfortunately cannot be solved in closed-form, but through a line-search algorithm such as the Newton-Raphson method.

V. Numerical Results

In this section, we present some numerical results to illustrate our analytical findings. We refer to [9] and [14] for the system parameters for the 4×4 macro, and set $P_{ID} = 139$ W, $P_A = 742.2$ W, $\beta_1 = \beta_2 = 1$, $\lambda = 0.1$ s^{-1}, $\rho = 0.1$, such that $h_B = 1$ s.

In Fig. 3, we plot the average total power consumption for various values of θ (i.e., ratio of actual sleep period to the transition latency/set-up time) and η (i.e., ratio of component activation latency to the deactivation latency). We observe that increasing θ leads to reduction in the average power consumption since more time will be spent in the actual sleep and less overhead power consumption during the activation and deactivation phases.

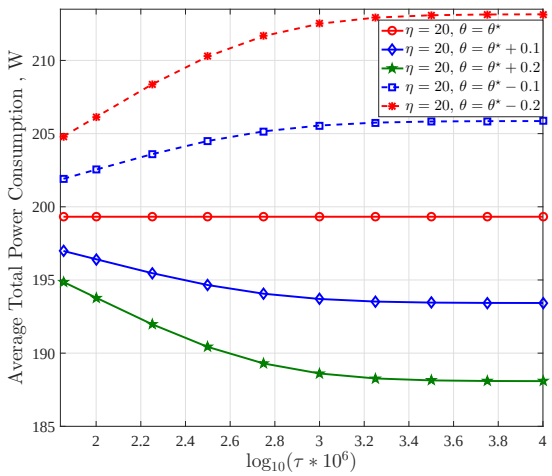

Fig. 4. Effect of the increasing/decreasing $\theta^\star$ on the average total power consumption.

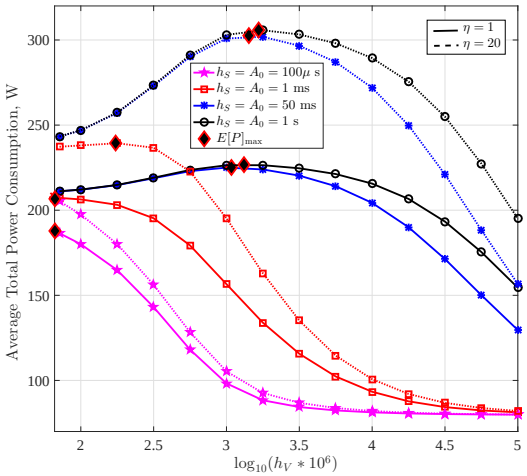

Fig. 5. Effect of the deactivation and activation latency for fixed transition latency/set-up time $A_0 = h_{SA} + h_{SD}$. $h_V^\star$ is shown with the diamond marker.

In addition, it also shifts the average power curve towards the ideal case, which does not consider the overhead cost associated with component activation and deactivation. Furthermore, for the same θ, increasing η leads to an increase in the average total power consumption. This is due to the fact that more power is consumed during the component activation phase than the component deactivation phase. Moreover, it can be seen that in the considered scenario, where the $\theta \geq 2$, the average total power consumption is strictly decreasing with the sleep depth. It can also be observed that when the actual sleep period is significantly higher than the set-up time, e.g., $\theta = 20$, then η has a marginal impact on the average total power consumption. On the other hand, the effect of η becomes significant when the actual sleep period is comparable to the set-up time, e.g., $\theta = 2$. This suggests a careful selection of the components to be deactivated/activated when the actual sleep period is comparable to the set-up time, while a relaxed selection criteria can be followed when θ is large. In Fig. 3, we also benchmark our results with the case with fixed power consumption for all sleep depth ($P_{SL} = 86.3$ W) and during the transition phase ($P_{SD} = P_{SA} = 2P_{ID}$). It can be seen that the fixed power consumption approach leads to an overestimation of the average total power consumption.

In Fig. 4, we plot the average total power consumption for a fixed $\eta = 20$ while varing θ around $\theta^\star \approx 0.9286$ when $\beta_1 = \beta_2 = 1$. As observed earlier in our analysis, the average total power consumption remains constant for varying sleep depth τ when $\theta = \theta^\star$. It increases with τ when $\theta < \theta^\star$ and decreases with τ when $\theta > \theta^\star$.

In Fig. 5, we plot the average total power consumption for fixed transition latency/set-up time. It can be observed that the average power consumption decreases with the vacation time h_V when the set-up time is very short ($h_S = A_0 = 100$ μs). Whereas, for higher set-up time, there exists a vacation period $h_V^\star$ such that the average total power increases over $h_V \in [0, h_V^\star]$ and decreases over $h_V \in [h_V^\star, +\infty]$. Note that in order to take into consideration the change in the BS state, the activation and deactivation power consumption as expressed in (3) and (4), respectively depends on the sleep depth. Hence, for a fixed set-up time, the set-up power consumption increases as the actual sleep time increases. Consequently, the average total power consumption first increases until the point where the gains from the lower power consumption due to the deeper sleep level becomes predominant.

VI. Conclusions

In this paper, we have investigated the impact of BS's component deactivation and activation times (transition latency) on the average total power consumption. We utilized the curve fitting approach to model the power consumed during the sleep level as a function of the BS's sleep depth. Numerical results showed a close match between our proposed approach and the actual sleep mode power consumption for selected base station types. Next, we analyzed the optimal sleep depth of the base station, taking into consideration the increased power consumption during base station activation, which exceeds the no load power consumption, and the power consumed during base station deactivation process, which also exceeds the power consumed when the actual sleep level is attained. Results showed that the average total power consumption monotonically decreases with the BS sleep depth as long as the ratio of the actual sleep period to the transition latency/set-up time exceeds a certain threshold. Furthermore, for a fixed transition latency, there exits a BS sleep depth that maximizes the average power consumption.

ACKNOWLEDGEMENT

This work was supported in part through ESPRC UK Global Challenges Research Fund (GCRF) allocation under grant no. EP/P028764/1, and in part by Huawei under the project: Energy-Proportional eNodeB for LTE-Advanced and Beyond.

REFERENCES

[1] J. G. Andrews et al., "What will 5G be?" *IEEE Journal on Selected Areas in Communications*, vol. 32, no. 6, pp. 1065–1082, Jun. 2014.

[2] B. Evans, O. Onireti, T. Spathopoulos, and M. A. Imran, "The role of satellites in 5G," in *23rd European Signal Processing Conference (EUSIPCO)*, Aug 2015, pp. 2756–2760.

[3] Nokia Siemens Networks, ETSI RRS05-024, 2011.

[4] O. Arnold, F. Richter, G. Fettweis, and O. Blume, "Power consumption modeling of different base station types in heterogeneous cellular networks," in *Proc. Future Network and Mobile Summit*, Florence, Italy, Jun. 2010.

[5] G. Auer et al., "D2.3: Energy efficiency analysis of the reference systems, areas of improvement and target breakdown," INFSO-ICT-247733 EARTH (Energy Aware Radio and NeTwork TecHnologies), Tech. Rep., Nov. 2010.

[6] G. Auer et al., "How much energy is needed to run a wireless network?" *IEEE Wireless Communications Magazine*, vol. 18, no. 5, pp. 40–49, Oct. 2011.

[7] C. Desset et al., "Flexible power modeling of LTE base stations," in *IEEE Wireless Communications and Networking Conference (WCNC)*, 2012, pp. 2858–2862.

[8] C. Desset, B. Debaillie, and F. Louagie, "Modeling the hardware power consumption of large scale antenna systems," in *IEEE Online Conference on Green Communications*, Nov 2014.

[9] B. Debaillie, C. Desset, and F. Louagie, "A flexible and future-proof power model for cellular base stations," in *IEEE Vehicular Technology Conference (VTC Spring)*, 2015.

[10] A. Mohamed, O. Onireti, M. A. Imran, A. Imran, and R. Tafazolli, "Control-data separation architecture for cellular radio access networks: A survey and outlook," *IEEE Communications Surveys & Tutorials*, vol. 18, no. 1, pp. 446–465, Firstquarter 2015.

[11] E. Ternon, P. K. Agyapong, and A. Dekorsy, "Performance evaluation of macro-assisted small cell energy savings schemes," *EURASIP Journal on Wireless Communications and Networking*, vol. 2015, no. 1, p. 209, 2015. [Online]. Available: http://dx.doi.org/10.1186/s13638-015-0432-0

[12] X. Guo, Z. Niu, S. Zhou, and P. R. Kumar, "Delay-constrained energy-optimal base station sleeping control," *IEEE Journal on Selected Areas in Communications*, vol. 34, no. 5, pp. 1073–1085, May 2016.

[13] X. Guo, S. Zhou, Z. Niu, and P. R. Kumar, "Optimal wake-up mechanism for single base station with sleep mode," in *25th International Teletraffic Congress (ITC)*, Sept 2013.

[14] IMEC, "Power model for today's and future base stations," [Online]. Available: http://www.imec.be/powermodel [Accessed:30 - Jan - 2017].

[15] B. H. Stark, G. D. Szarka, and E. D. Rooke, "Start-up circuit with low minimum operating power for microwatt energy harvesters," *IET Circuits, Devices Systems*, vol. 5, no. 4, pp. 267–274, Jul 2011.

[16] L. Wang, X. Feng, X. Gan, J. Liu, H. Yu, and D. Zhang, "Small cell switch policy: A consideration of start-up energy cost," in *IEEE/CIC International Conference on Communications in China (ICCC)*, Oct 2014, pp. 231–235.

[17] 3GPP, "Evolved Universal Terrestrial Radio Access (E-UTRA); Base Station (BS) radio transmission and reception," Technical Specification, April 2011, 3GPP TS 36.104 version 10.2.0 Release 10.

[18] D. Ferling et al., "D4.3: Final report on green radio technologies," INFSO-ICT-247733 EARTH (Energy Aware Radio and NeTwork TecHnologies), Tech. Rep., Jun 2012.

[19] N. C. Beaulieu and F. Rajwani, "Highly accurate simple closed-form approximations to lognormal sum distributions and densities," *IEEE Communications Letters*, vol. 8, no. 12, pp. 709–711, Dec. 2004.

[20] S. M. Ross, *Introduction to Probability Models*. Academic Press, 1997.